16TH EUROPEAN CONFERENCE ON EARTHQUAKE ENGINEERING
THESSALONIKI 18 - 21 JUNE 2018

A COMPARATIVE STUDY ON THE PERFORMANCE OF SEMI-ACTIVE AND PASSIVE CONTROL SYSTEMS FOR MULTI-SPAN BRIDGES

B NEETHU[1], Diptesh DAS[2]

ABSTRACT

The present study investigates the performance of a semi-active and a passive controller for seismic response reduction of a multi-span bridge. A passive seismic isolation system using lead rubber bearing is developed for a multi-span bridge. Further a semi-active control scheme using magneto-rheological damper is developed. It is observed that one of the major problems in developing any structural control system is due to the presence of uncertainties and imprecision associated with noisy and faulty input measurements, system parameter values and possible changes to the system. The present study focuses on developing a robust control system, which can treat the system uncertainties and imprecision effectively. A continuous sliding mode control algorithm, is adopted due to its inherent stability and distinguished robustness to system parameter variation and external disturbances. The performance of the passive and semi-active controllers are evaluated for a multi-span bridge subjected to various real earthquake ground motions.
On investigating the performance of the control systems, the results show that, both the controllers are effective in controlling the seismic responses of the bridge. However, the deck displacement responses are observed to be high in case of near field earthquakes for the passive control. The semi-active control strategy is efficient in reducing all the seismic responses of the bridge. Numerical results indicate that the response quantities of the bridge with the semi-active controller can be reduced to a satisfactory level, superior to those of the passive controller. The controller also shows a stable and robust performance for all the earthquakes.

Keywords: magneto-rheological damper; passive control; semi-active control; earthquake; sliding mode control.

1. INTRODUCTION

Bridges are generally recognized as a significant component of the transportation system. During any natural calamities bridges form a vital component in managing emergencies. Historically examples of catastrophic failure of bridges are reported during earthquakes all over the world. Although considerable progress has been achieved in the design and construction of earthquake resistant bridges, there are many gap areas which still remain unexplored in understanding the seismic behavior of bridges.
The dominant periods of regular earthquake accelerations are found to be about 0.1 to 1 secs. The range 0.2 to 0.6 secs is reported to have the maximum severity. Considering this aspect, bridges are more vulnerable when subjected to severe earthquakes as majority of the bridges have their fundamental natural period in the range of 0.2 to 1.2 secs. The conventional methods of design in which the bridges are designed to resist a severe earthquake elastically are recognized to be uneconomical. Structural vibration control methods can be one of the most promising alternatives in this regard. Most of the researchers have investigated the structural control systems for building structures. In contrast, the vibration control techniques have not been investigated to the same extent for bridges. Bridges being more vulnerable to earthquakes more attention need to be paid on protection of bridges against seismic attacks. Evidence justifying the need for structural control systems is

[1]Research Scholar, National Institute of Technology Durgapur, India, neethunitdgp@gmail.com
[2]Assistant Professor, Department of Civil Eng., NIT Durgapur, India, d_diptesh@yahoo.com

provided in numerous literature.

Seismic isolation is an effective and promising structural control method for bridges as it reduces the forces on bridges by lengthening the fundamental period of the bridge, and by increasing the energy dissipating capacity. Numerous studies had been done in this area and seismic isolation is found to be one of the most successful techniques to mitigate the risk to life and property during strong earthquakes(Skinner et al. 1993). Seismic isolation introduces a flexible layer between the super-structure and foundation and thereby de-couples the structure from the vibrational energy. Amongst all the isolators, elastomeric base isolation system is most widely used for seismic protection of structures. The Lead Rubber Bearing (LRB) which is a modified version of the basic laminated rubber bearing is considered for the present study.

The present study focuses on the use of lead rubber bearings for the seismic isolation of multi-span bridges. Numerous studies on the use isolation systems for seismic response reduction of structures are reported in literature. (Chen and Liu 2009; Ghobarah and Ali 1988; Jangid 2008; Patil and Reddy 2012; Vasiliadis 2016). The studies have also brought out some of the drawbacks of seismic isolation such as the displacement responses at the level of isolation is usually seen to be high for near-field earthquakes. (Skinner et al. 1993). A usual method to reduce these displacements is by increasing the damping. However, this may increase the internal deformation and the absolute accelerations of the superstructure, thus defeating many of the gains for which base isolation is intended (Naeim and Kelly 1999). It is also observed that passive-device methods are unable to adapt to structural changes and to varying usage patterns and loading conditions. However, semi-active systems have the advantage of adaptability which can be ensured by adopting a suitable control algorithm which can accommodate the uncertainties and imprecisions.

Semi-active control systems have the major advantages of versatility and adaptability of active control systems, without requiring large energy supply, but having the reliability of passive control system(Lee and Kawashima 2007). Among the different semi-active devices, Magneto-rheological (MR) damper, which is a reliable and fail-safe device, has attracted significant attention recently due to its high dynamic range and less power consumption. The use of MR dampers for the vibration control of bridges are studied by researchers like (Jung et al. 2003; Lee and Kawashima 2007; Lee et al. 2008; Sahasrabudhe and Nagarajaiah 2005). All these studies show that semi-active control using MR damper provides a feasible control method for mitigating seismic responses of bridge structures.

Furthermore, developing a mathematical model of a real structure-controller system accurately considering various parameter uncertainties involved in the process is a difficult task. The problem is more critical for semi-active control of bridges due to the involvement of non-linear dynamics of MR damper. Hence, the control systems should be able to accommodate noisy input measurements, uncertainty in system parameter values and possible changes to the system. These problems, however, need to be tackled in order to design and develop controllers which will efficiently perform for such complex systems.

Different control strategies are reported in the literature such as the linear quadratic regulator (LQR), linear quadratic Gaussian (LQG) controller, fuzzy logic, neural network, sliding mode algorithm instantaneous optimal control, etc. Compared to all the algorithms, the sliding mode control (SMC) algorithm can accommodate uncertainty and imprecision more effectively due to its inherent robustness and ability to cope with the parameter uncertainties and imprecisions. SMC algorithm using MR dampers has been effectively used for seismic control of structures. However, relatively less studies are reported on the application to bridge structures. In the present study, a continuous SMC algorithm (using MR damper), which does not have any chattering effect, is adopted. It has inherent stability and distinguished robustness to system parameter variation and external disturbances. Although extensive research has been carried out in the area of structural control relatively less work is reported on the control schemes based on sliding mode control (SMC) algorithm for bridge structures using MR dampers.

The overall objective of the study is to investigate the performance of a passive (LRB based seismic isolation system) and semi-active control (sliding mode control using MR damper) in reducing the seismic responses of a three-span bridge subjected to various earthquake ground motions. In order to study the effectiveness of the controller, the performance of the controllers had been investigated for fourteen different earthquake ground motion records. The earthquakes are chosen in such a way that all possible characteristic variations can be accommodated. Out of these fourteen earthquakes, seven are near-field and seven are far-field.

2. THEORETICAL DEVELOPMENT

This study investigates the performance of a three-span continuous bridge. The theoretical development of the structure-controller involves mathematical modelling of the bridge, isolator, damper and the controller. The numerical simulations of the dynamic responses of the bridge, subjected to various near filed and far filed earthquakes, are carried out using a full-state feedback control loop. MATLAB, Simulink, and a complementary set of toolboxes are used to conduct numerical simulation and computations in the work that follows.

2.1 Modeling of the bridge

The seismic response and performance of a three-span continuous bridge is investigated. The schematic diagram of the three-span bridge considered in the study is shown in Figure.1a. A simplified model for the deck-pier system attached with MR damper is shown in Figure.1b. The equivalent mechanical model for the same is depicted in Figure.1.c. The pier is discretized into number of nodes with lateral degrees of freedom (as in shear building) and the bridge deck is treated as rigid mass. The piers and superstructure are assumed to remain elastic. This model has been also used in literatures like (Ghobarah and Ali 1988; Jangid 2008; Wang et al. 1998).

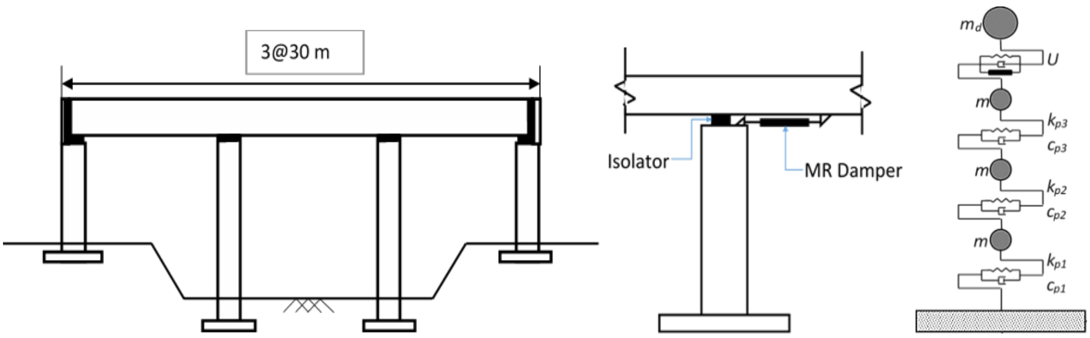

(a) (b) c)

Figure. 1 (a). Three-span bridge deck-pier system, (b). Simple structural model for deck-pier system attached with control devices and (c). Equivalent mechanical model

The governing equation of motion for the bridge subjected to ground motion is expressed in matrix form as:

$$[\boldsymbol{M}]\{\ddot{\boldsymbol{X}}\}+[\boldsymbol{C}]\{\dot{\boldsymbol{X}}\}+[\boldsymbol{K}]\{\boldsymbol{X}\}+[\boldsymbol{D}]\{\boldsymbol{F}\}=-[\boldsymbol{M}][\boldsymbol{r}]\{\ddot{\boldsymbol{X}}_g\} \tag{1}$$

where **[M], [C]** and **[K]** are mass, damping and stiffness matrices, respectively, of the bridge structure of the order [4×4]; $\{\boldsymbol{X}\}=\{\boldsymbol{X}_1, \boldsymbol{X}_2 \ldots \boldsymbol{X}_{n,} \boldsymbol{X}_d\}^T$, $\{\boldsymbol{X}\},\{\dot{\boldsymbol{X}}\},\{\ddot{\boldsymbol{X}}\}$ are structural displacement, structural velocity and structural acceleration vectors, respectively; X_d is the displacement of the bridge deck relative to ground; **[D]** is the location matrix for the restoring forces of control device; **{F}** is vector containing the restoring forces; **{r } = {1,1,.........,1 }$^{\mathbf{T}}$** is influence coefficient vector and $\{\ddot{\boldsymbol{X}}_g\}$ is earthquake ground acceleration.

The equations of motion is solved using the state-space form:

$$\dot{\boldsymbol{z}}(\boldsymbol{t}) = \boldsymbol{A}\boldsymbol{z}(\boldsymbol{t}) + \boldsymbol{B}\boldsymbol{u}(\boldsymbol{t}) + \boldsymbol{H}\boldsymbol{f}(\boldsymbol{t}) \tag{2}$$

where $\boldsymbol{z}(\boldsymbol{t}) = \begin{bmatrix} \boldsymbol{x}(\boldsymbol{t}) \\ \dot{\boldsymbol{x}}(\boldsymbol{t}) \end{bmatrix}$ is the 2n-dimensional state vector, where n=4

$\boldsymbol{A} = \begin{bmatrix} 0 & \boldsymbol{I} \\ -\boldsymbol{M}^{-1}\boldsymbol{K} & -\boldsymbol{M}^{-1}\boldsymbol{C} \end{bmatrix}$ is the [2n ×2n] system matrix, and

$\boldsymbol{B} = \begin{bmatrix} 0 \\ \boldsymbol{M}^{-1}\boldsymbol{D} \end{bmatrix}$ and $\boldsymbol{H} = \begin{bmatrix} \boldsymbol{I} \\ \boldsymbol{M}^{-1}\boldsymbol{E} \end{bmatrix}$ are [2n × r] and [2n × 1] location matrices specifying respectively, the locations of controllers and external excitations in the state-space. 0 and I denote respectively, the null matrix and the identity matrix of appropriate dimensions".

2.2 Modelling of the Lead Rubber Bearing (LRB)

The LRB isolator is a multi-layered laminated rubber bearing along with a central lead-core to add damping to the isolation system. The LRB isolator provides the combined features of vertical load support, horizontal flexibility, restoring force and damping in a single unit. The ideal force-deformation behavior of the LRB system is generally represented by non- linear characteristics following a hysteretic nature. The LRB follows a non-linear hysteretic force-deformation behaviour which is characterised by the characteristic yield strength (Q_d), post-yield stiffness (k_b) and yield displacement (q).The mathematical modelling of the is done with the help of a non-linear Wen's (Wen 1976) model to characterize the hysteretic behaviour of the LRB systems. The restoring force developed in the isolation bearing is given by,

$$F_b = c_b \ddot{x}_b + \alpha k_b x_b + (1-\alpha) Q_d Z \tag{3}$$

where, Q_d is the yield strength of the bearing; α is an index which represent the ratio of post to pre-yielding stiffness; k_b is the initial stiffness of the bearing; c_b is the viscous damping of the bearing; and Z is the non-dimensional hysteretic displacement component satisfying the following non-linear first order differential equation expressed as,

$$q\dot{Z} = A\dot{x}_b - \beta |\dot{x}_b| z |z|^{n-1} - \tau x_b |z|^n \tag{4}$$

where, q is the yield displacement; dimensionless parameters β, τ, A and n are selected such that predicted response from the model closely matches with the experimental results (Constantinou and Tadjbakhsh 1985). The parameter n is an integer constant, which controls smoothness of transition from elastic to plastic response. The parameters α, β, τ and A are dimensionless. The values of the parameters have to be selected appropriately for the modelling. The isolation properties are generally designed to specified values of the parameters such as: isolation period, $T_b = 2\pi\sqrt{\frac{M}{k_b}}$, and the normalized yield strength, $F_o = \frac{Q_d}{W}$ and damping ratio $\xi_b = \frac{c_b}{2M\omega_b}$.

2.3 Modeling of M R Damper

Several models have been proposed to describe the behavior of the MR damper. The present study uses the Bouc-Wen model of the MR damper (Yoshida et al. 2003). The equation for the force of the system is given by:

$$f = c_0 \dot{q} + \alpha z \tag{5}$$

where, $\dot{z} = -\gamma \mid \dot{x} - \dot{y}|z||z|^{n-1} - \beta(\dot{x} - \dot{y})|z|^n + A(\dot{x} - \dot{y})$ (6)

By adjusting the parameters of the model γ, β, and A, one can control the shape of the hysteresis loops for the yielding element. The following equations account for the dependence of the force on the voltage applied to the current driver and the resulting magnetic current:

$$\alpha = \alpha(u) = \alpha_a + \alpha_b u \quad (7)$$

$$c_1 = c_1(u) = c_{1a} + c_{1b}u \quad (8)$$

$$c_0 = c_0(u) = c_{0a} + c_{0b}u \quad (9)$$

where u is the output of a first-order filter given by

$$\dot{u} = -\eta(u - v) \quad (10)$$

In the above equation, v is the commanded voltage sent to the current driver. Eq. (14) is necessary to model the dynamics involved in reaching rheological equilibrium and in driving the electromagnet in the MR damper. Other parameters are fixed coefficients that are calculated by adjusting the behavior of MR damper and are to be obtained based on the laboratory experiment.

2.4 Semi-active Control Algorithm

A schematic representation of the structure-controller system is shown in Figure 2. The MR damper produces the control force based on the seismic responses of the structure. The optimal control force and the voltage required for damper operation is determined by the controller. The controller performs the operation in two stages:

Stage 1: Based on the full-state feedback of the structural responses and the earthquake excitation, the sliding mode algorithm(Yang et al. 1994) calculates the desired optimal control force required to drive the state trajectories on to a sliding surface, where the motion is stable.

The fundamental condition to operate the MR damper is based on a generated damping force that is related to the input voltage. The sliding mode control algorithm is selected so that the damping force can track a desired command damping force. In sliding mode control, the aim of the control force is to drive the response trajectory toward the sliding surface, where the motion on the sliding surface defined by S = 0 is stable, and then to maintain it on the sliding surface. The basic concept of this theory is to design a controller such that the motion of the system tends to sliding mode surface. The design of a sliding mode controller consists of two steps: the design of the sliding surface and the design of the control strategy to steer the state trajectory to the sliding surface(Yang et al. 1994).

Stage 2: The controller calculates the command voltage to be applied to the MR damper for a given displacement and velocity based on the desired optimal force and the force available from the MR damper at the previous time step. The clipped optimal algorithm(Dyke and Spencer, B.F. 1997) is used for this purpose.

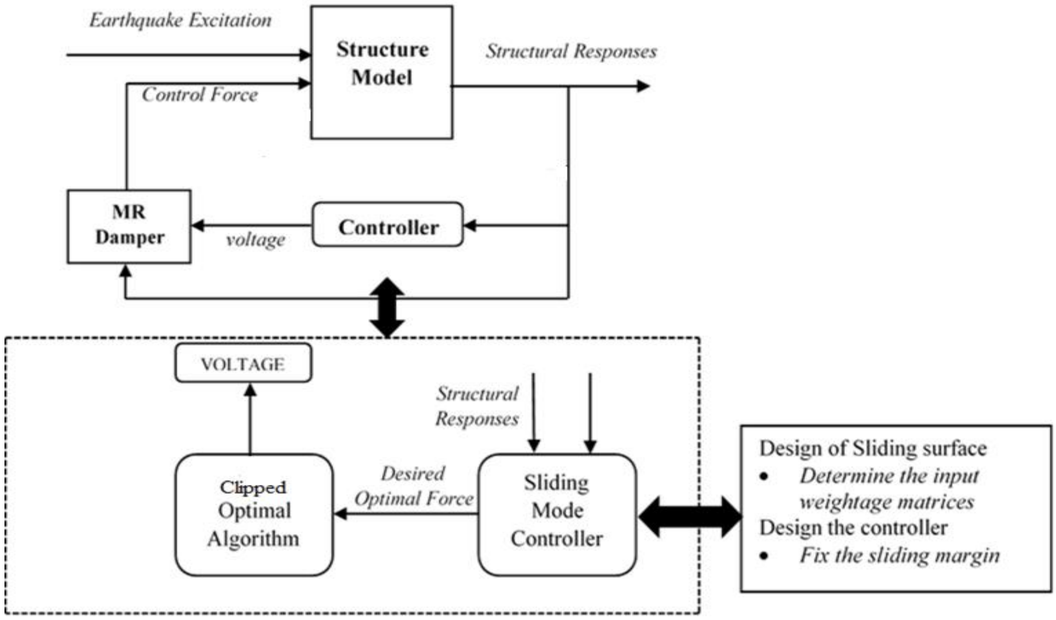

Figure 2. Schematic of Semi-active control System

3. NUMERİCAL STUDY

The effectiveness of the proposed hybrid control algorithm is studied by considering a three -span bridge structures subjected to various real earthquake ground motions. The details of the bridge is taken from literature (Wang et al. 1998). The properties are: deck mass = 771.12×10^3 kg; mass of each pier = 39.26×10^3 kg; moment of inertia of piers = 0.64 m^4; Young's modules of elasticity = 20.67×10^9 (N/m^2); pier height = 8 m; and total length of bridge = 90 m. The fundamental time period of the bridge is 0.45 sec. The seismic response of the bridge and the effectiveness of the control are investigated for seven far-field (FF) and seven near-field (NF) earthquake ground motions. The near-field earthquake ground motions considered are: Kobe, Northridge, Chichi, Tabas, Morgan Hill, Loma Prieta and El. Centro. The far-field earthquake ground motions considered are Imperial Valley, Coalinga, San Fernando, Victoria Mexico, Whitter Narrows, Chaflant, Landers. Table 1 shows the details of the ground motion characteristics and the earthquake data is taken from PEER ground motion database. For the seismic response analysis, all the ground motions are scaled to 0.3g.

Table 1. Earthquake ground motion properties.

Earthquake	Mw	Station	Dist(km)	PGA(g)	PGV(cm/s)
Imperial Valley	6.5	Coachella Canal #4	50.1	0.115	12.47
Coalinga	6.4	Parkfield- Cholame	55.77	0.039	4.22
San Fernando	6.6	2516 Via Tejon PV	55.2	0.025	3.82
Victoria Mexico	6.3	SAHOP Casa Flores	39.3	0.101	7.77
Chalfant Valley	6.2	Convict Creek, 90	31.19	0.071	3.84
Whittier	6	Canyon Country	48.18	0.109	7.32
Landers	7.3	Baker Fire Station	87.94	0.107	9.32
Kobe	6.9	KJMA	18.27	0.831	95.75
Chichi	7.62	TCU065	26.67	0.831	129.55
Northridge	6.69	LA DAM	11.79	0.576	77.09
Tabas	7.35	Tabas	55.24	0.851	121.22
Morgan hill	6.19	Anderson dam	16.67	0.449	29.01
Loma Prieta	6.9	LGPC	3.5	0.57	102.01
Petrolia	7	El Centro Array 9	12.99	0.31	30.

In order to choose the optimum parameters for the isolation system, in the preliminary study(Neethu and Das 2015), a rigorous parametric study was conducted to find the parameters for getting maximum response control. The LRB parameters selected for the present study are T_b =2.5sec, F_o= 0.30, ξ_b= 0.10 and α= 0.1. An MR damper of 1000 kN capacity and a maximum input voltage of 10V is used for the present study. The damper parameters used here as per (Yoshida and Dyke 2004). The parameters for the dynamic model that were determined to best fit the data based on the experimental results of a 1000 KN damper are $C_{o\alpha}$ =4.40 Ns/cm, C_{ob}=44.0Ns/(cm V), A=1.2, β,γ=3 cm^{-1}, α_a =1.08728×10^5 N/cm, α_b =4.9616×10^5 N/(cm V), n=1, η=50 s^{-1}.

4. RESULTS AND DISCUSSION

In this study, a multi-span bridge is selected from the literature (Wang et al. 1998) and a lumped mass model of the bridge is numerically modeled using Matlab. To study the performance of the control system, the responses of the bridge, namely, deck displacement, deck acceleration and base shear, are considered.

4.1 Passive Control.

In order to study the performance of the LRB, the responses of the isolated bridge, subjected to fourteen different near-field and far-field earthquake ground motions, are compared with those of non-isolated bridge. The variation of the responses namely maximum isolator displacement, deck acceleration and base shear are considered in evaluating the performance.

Table 2 shows the absolute maximum values of the responses of the isolated and uncontrolled bridge. The percentage control for each response is calculated which indicates the percentage reduction of response quantities (displacement, acceleration and base shear) of the isolated structure with respect to those of the non-isolated structure. The mean of the percentage control of responses is found for all the responses for the set of 14 earthquakes. The maximum average percentage control of 47 % is observed for the acceleration responses. The efficiency of the isolator in controlling the displacement responses is less when compared to the deck acceleration and base shear responses. The results also show that for some near field earthquakes like the Northridge and Petrolia the displacement responses are increased leading to a negative percentage control of -23% and -9% respectively.

Table 2: Percentage control of responses of the isolated bridge

Earthquakes	**Deck Displacement (mm)**		**% Control**	**Deck Acceleration (m/s^2)**		**% Control**	**Base shear (W_d)**		**% Control**	**Avg. % Control**
	UC	**LRB**		**UC**	**LRB**		**UC**	**LRB**		
Imperial Valley	34.55	30.77	11	6.53	3.42	48	0.70	0.36	49	36
Coalinga	31.85	23.00	28	6.00	3.32	45	0.65	0.39	40	38
San Fernando	25.71	15.59	39	4.89	2.05	58	0.52	0.23	57	51
Victoria Mexico	23.41	15.38	34	4.47	1.91	57	0.49	0.21	57	49
Whitter Narrows	27.24	15.54	43	5.18	1.97	62	0.55	0.25	55	**53**
Chaflant	23.66	15.86	33	4.54	1.85	59	0.48	0.21	56	49
Landers	16.91	11.88	30	3.21	1.64	49	0.34	0.20	41	40
Kobe	35.11	23.06	34	6.55	2.94	55	0.72	0.35	52	47
Northridge	19.25	23.59	-23	3.66	3.26	11	0.40	0.36	10	1
Chichi	12.90	12.35	4	2.41	1.89	21	0.27	0.23	15	14
Tabas	28.71	22.42	22	5.49	2.54	54	0.58	0.27	53	43
Morgan Hill	30.72	11.90	61	5.80	1.34	77	0.63	0.14	77	**72**
Loma Prieta	41.88	41.61	1	7.87	4.70	40	0.86	0.53	39	27
Petrolia	20.23	28.08	-9	3.79	3.62	31	0.42	0.39	33	18
Average			**22**			**48**			**45**	

Figure 3 compares the time histories of the responses of the isolated bridge with the uncontrolled bridge subjected to Northridge earthquake ground motion (far-field). The acceleration response and base shear response are seen to be reduced more for the isolated bridge however, the displacement responses increase for the isolated bridge. This is due to the increased flexibility of the structure due to isolation. The figure shows that for the isolated bridge has a residual displacement of around 2.5 mm when subjected to the Northridge earthquake. It is important to note that this type of residual displacement may cause a permanent increase in the size of the thermal expansion gap and may render the bridge unusable.

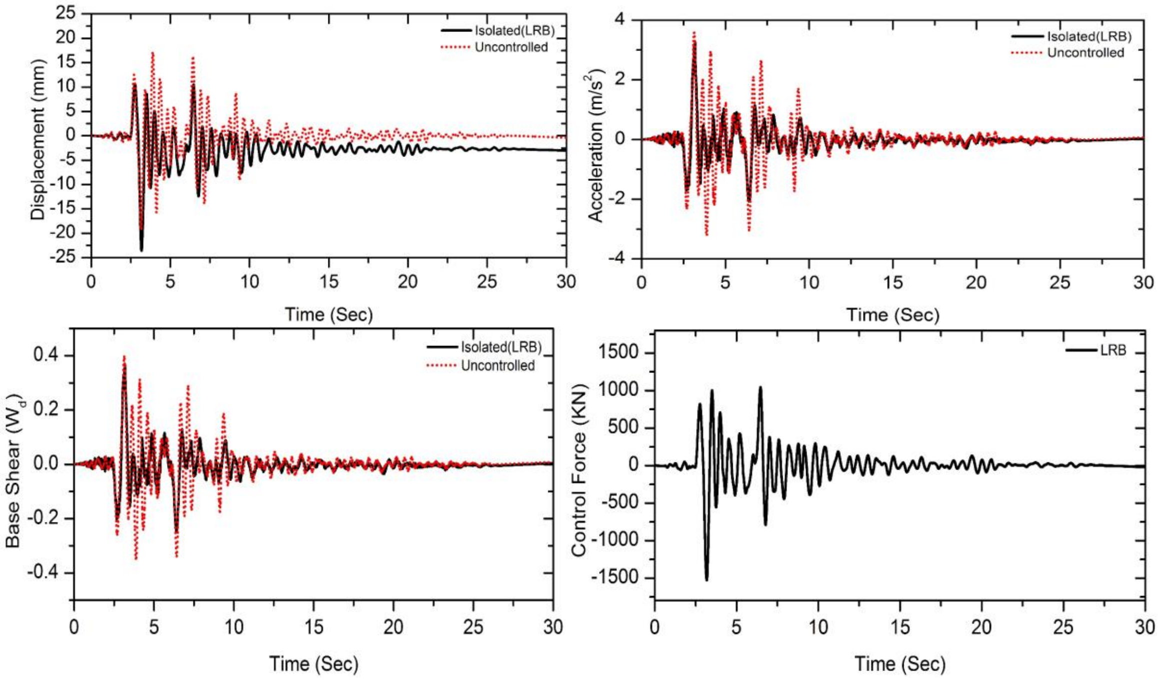

Figure 3: Time history responses (uncontrolled and controlled) of isolated bridge subjected to Northridge earthquake

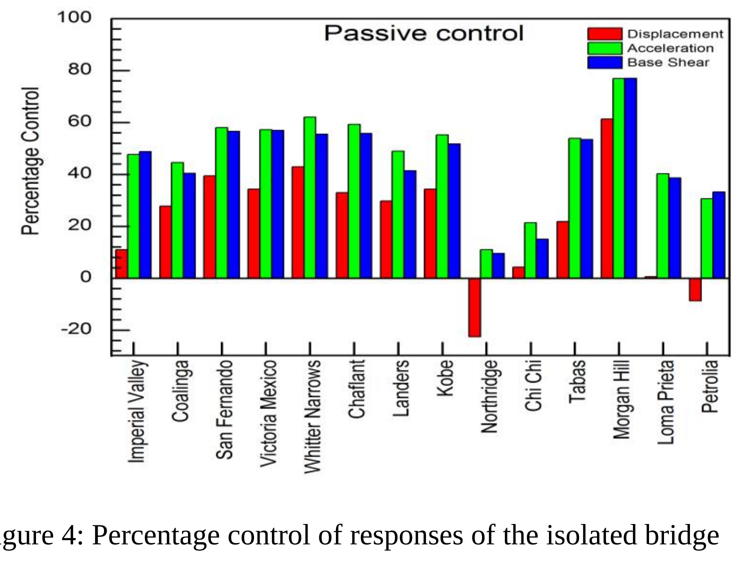

Figure 4: Percentage control of responses of the isolated bridge

Figure 4 shows the percentage control of the responses of the isolated bridge subjected to different earthquake ground motions. The results indicate that the isolation system is effective in reducing the deck acceleration and base shear for both far field and near field earthquakes. Maximum control of 61% for deck displacement and 77% for deck acceleration and base shear is observed for Morgan Hill earthquake. Similarly the lowest percentage control is observed for Northridge earthquake. The percentage control however, is different for different earthquakes and hence, it can be inferred that the performance of the isolator depends on the ground motion characteristics.

4.2 Semi-active Control

In order to study the performance of the semi-active controller, the responses of the controlled bridge, subjected to fourteen different earthquake ground motions, are compared with those of uncontrolled bridge. Table 3 shows the absolute maximum values of the responses of the controlled and uncontrolled bridge and the percentage percentage control for each response. The mean of the percentage control of responses is found for all the responses for the set of 14 earthquakes. The maximum average percentage control of 50 % is observed for the displacement responses followed by 49% for deck acceleration and 46% for base shear. The results show that all the responses are controlled efficiently both for near-field and far-field earthquakes.

Table 3: Percentage control of responses of the clipped optimal sliding mode based controller.

Earthquakes	**Deck Displacement (mm)**		**% Control**	**Deck Acceleration (m/s^2)**		**% Control**	**Base shear (W_d)**		**% Control**	**Avg. % Control**
	UC	**SMC**		**UC**	**SMC**		**UC**	**SMC**		
Imperial Valley	34.55	12.23	65	6.53	1.03	84	0.70	0.15	78	76
Coalinga	31.85	15.71	51	6.00	2.97	50	0.65	0.34	47	49
San Fernando	25.71	14.53	43	4.89	2.75	44	0.52	0.31	40	42
Victoria Mexico	23.41	11.88	49	4.47	2.65	41	0.49	0.31	37	42
Whitter Narrows	27.24	15.88	42	5.18	3.07	41	0.55	0.35	36	39
Chaflant	23.66	11.91	50	4.54	2.50	45	0.48	0.29	39	44
Landers	16.91	8.76	48	3.21	2.34	27	0.34	0.17	50	42
Kobe	35.11	20.00	43	6.55	3.76	43	0.72	0.42	43	43
Northridge	19.25	9.97	48	3.66	2.93	20	0.40	0.23	43	37
Chichi	12.90	6.20	52	2.42	1.02	58	0.27	0.15	44	51
Tabas	28.71	13.11	54	5.49	2.77	50	0.58	0.32	44	49
Morgan Hill	30.72	13.43	56	5.80	2.98	49	0.63	0.35	45	50
Loma Prieta	41.88	20.80	50	7.87	3.93	50	0.86	0.43	49	50
Petrolia	29.60	16.13	45	5.53	1.16	79	0.61	0.34	44	56
Average			50			49			46	

Figure 5 compares the time histories of the responses of the semi-actively controlled bridge with the uncontrolled bridge subjected to Northridge earthquake ground motion (far-field). The displacement responses are seen to be reduced more for the controlled bridge when compared to the acceleration responses and base shear responses.

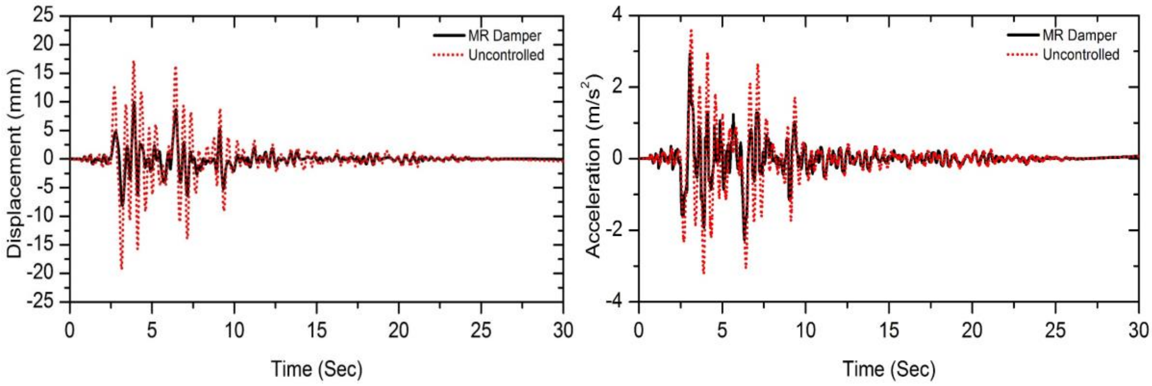

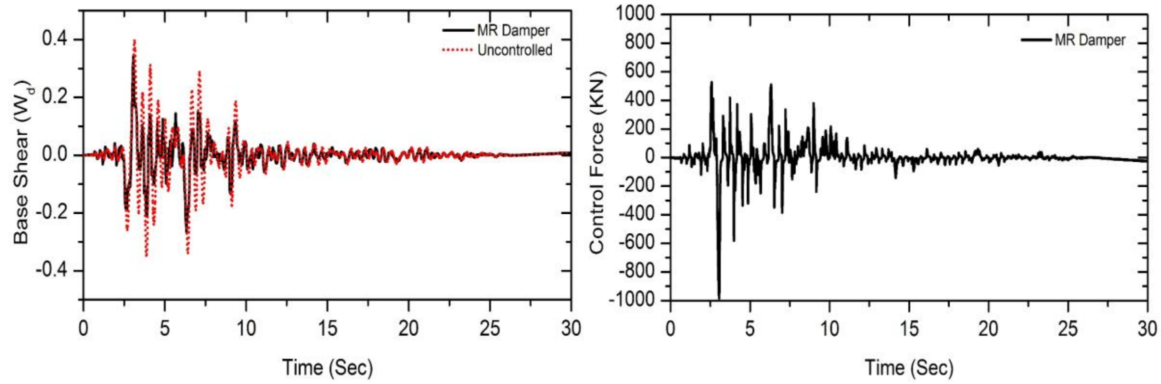

Figure 5: Time history responses (uncontrolled and controlled) of SMC based controller for the bridge subjected to Northridge earthquake

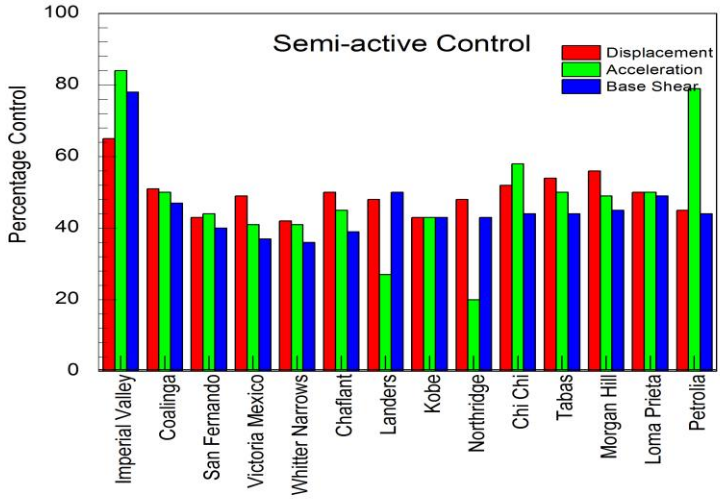

Figure 6: Percentage control of responses of the semi-active control based bridge

Figure 6 shows that the MR damper is more effective in controlling the deck displacement when compared to the deck acceleration. Maximum control of 65% for deck displacement, 84% for deck acceleration and 78% for base shear is observed for Imperial Valley earthquake. Similarly the lowest percentage control is observed for Northridge earthquake. The percentage control however, is different for different earthquakes and hence, it can be inferred that the performance of the controller depends on the ground motion characteristics.

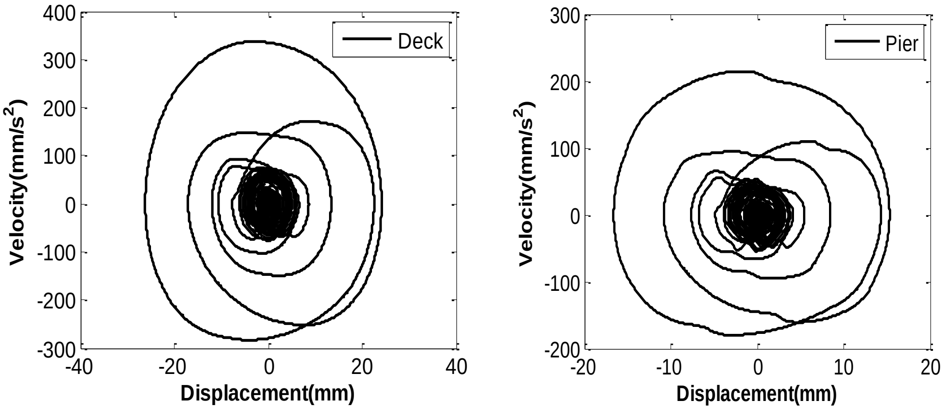

(a) (b)

Figure 7. Phase Plots for displacements of (a) deck and (b) pier top of the bridge for Northridge earthquake

The stability of the controller is studied with the help of the phase plots. The phase planes for the deck and pier top controlled by the SMC algorithm based controller are shown in Figures 7 (a) and 7 (b), respectively. It is observed from the resultant motion on the sliding surface or the phase plane trajectory plots that each of the trajectories slides towards its respective sliding surface (S=0) or the equilibrium point. The curves start from the initial value point, and converge to the stable points area around (0, 0) in a close-wise direction and thisconfirms that the closed-loop system is stable.

4.3 Comparison of performance of the controllers

The performance of the passive and semi-active controller is compared in terms of the percentage control of the different responses. Figure 8 shows the comparison of the percentage control of responses for the displacement, acceleration and base shear responses. The red line in each of the figure separates the set of near-field (left side of line) and far- field earthquakes (right side of line). The percentage control of displacement responses is very high for the semi-active controller when compared to the passive controller for both near-field as well as far-field earthquakes. The passive controller is not very effective in controlling the displacement responses under near-field earthquakes. In case of acceleration and base shear responses the performance of the passive control is better than the semi-active control for some of the near field earthquakes. On considering the overall performance, the semi-active controller is more efficient in controlling the responses for both near-field and far-field earthquakes with a much lower control force, as compared to the passive controller.

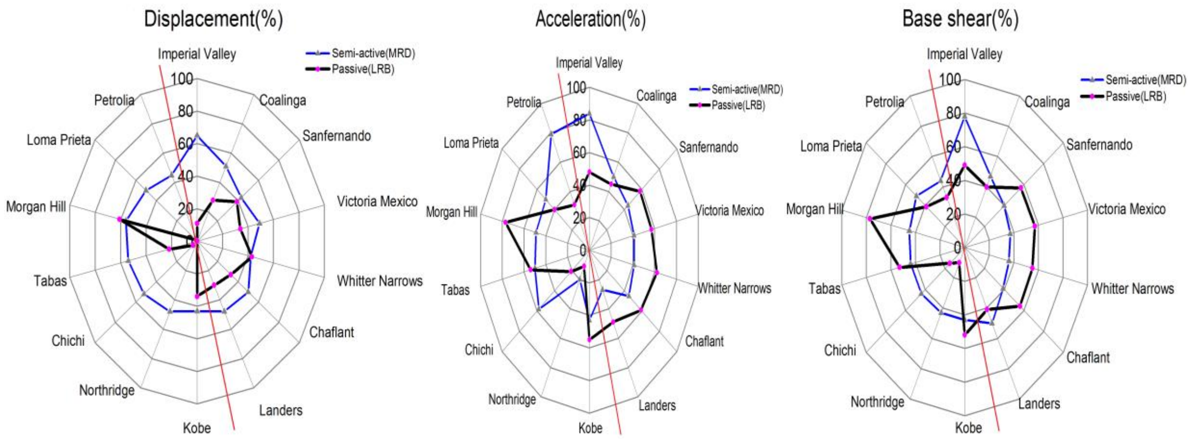

Figure 8 Comparison of Percentage control of responses for passive and semi-active controller.

5. CONCLUSIONS

In the present study a passive seismic isolation system using lead rubber bearing and a sliding mode based semi-active control scheme using magneto-rheological damper is developed for a three span bridge. The performance of both the controllers are analyzed and compared by considering different near-field and far-field earthquakes. Both the controllers are found to be effective in reducing the seismic responses of the bridge. On comparison of the performance the semi-active controller is found to be more effective in terms of response reduction as well as gives a robust performance for both near-field and far-field earthquake.

The passive control could effectively control all the responses of the bridge for far field earthquakes, however the deck displacement gets increased for some of the near field earthquakes resulting in residual displacements. The results shows that the isolated bridge has a residual displacement of around 2.5 mm when subjected to the Northridge earthquake which is a near field earthquake. It is important to note that this type of residual displacement may cause a permanent increase in the size of the thermal expansion gap and may render the bridge unusable.

The semi-active control effectively reduces all the responses for all the earthquakes. The phase plots for the deck and pier start from the initial value point, and converge to the stable points area around (0, 0) in a close-wise direction and this confirms that the closed-loop system is stable.

On considering the overall performance, the semi-active controller is more efficient in controlling the responses for both near-field and far-field earthquakes with a much lower control force, as compared to the passive controller. It is generally observed from the numerical results that the performance of the controller varies for different earthquake ground motion characteristics. Hence, more elaborate study is required to investigate the effect of different ground motion parameters on the seismic responses as well as the performance of the controller.

6. REFERENCES

Chen, C., and Liu, K. F. (2009). “Adaptive Fuzzy Sliding Mode Control for Seismically Excited Bridges with Lead Rubber Bearing Isolation.” *International Journal of Uncertainty*, 17(5), 705–727.

Constantinou, M. C., and Tadjbakhsh, I. G. (1985). “Hysteretic dampers in base isolation: random approach.” *Journal of Structural Engineering*, 111(4), 705–721.

Dyke, S. J., and Spencer, B.F., J. (1997). “A Comparison Of Semi-Active Control Strategies For The MR Damper.” *Proceedings Intelligent Information Systems. IIS’97*, (6), 580–584.

Ghobarah, A., and Ali, H. M. (1988). “Seismic performance of highway bridges.” *Engineering Structures*, 10, 157–166.

Jangid, R. S. (2008). “Equivalent linear stochastic seismic response of isolated bridges.” *Journal of Sound and Vibration*, 309(3–5), 805–822.

Jung, H.-J., Spencer, B. F., and Lee, I.-W. (2003). “Control of Seismically Excited Cable-Stayed Bridge Employing Magnetorheological Fluid Dampers.” *Journal of Structural Engineering*, 129(7), 873–883.

Kunde, M. C., and Jangid, R. S. (2003). “Seismic behavior of isolated bridges: A-state-of-the-art review.” *Electronic Journal of Structural Engineering*, 3, 140–170.

Lee, T., and Kawashima, K. (2007). “Semiactive Control of Nonlinear Isolated Bridges with Time Delay.” *Journal of Structural Engineering*, 133(2), 235–241.

Lee, T. Y., Kawashima, K., and Chen, P. C. (2008). “Experimental And Analytical Study On A Nonlinear Isolated Bridge Under Semiactive Control.” *The 14th World Conference on Earthquake Engineering*.

Naeim, F., and Kelly, J. M. (1999). “Design of Seismic Isolated Structures: From Theory to Practice. .” *John Wiley & Sons,Inc.*, New York(USA).

Neethu, B., and Das, D. (2015). “Influence of Passive Isolator Parameters on Seismic Response Control of Multi - Span Bridges.” *Inernational Journal of Scientific Research Publications*, 5(4), 1–10.

Patil, S., and Reddy, G. (2012). “State Of Art Review - Base isolation systems for structures.” *International Journal of Emerging Technology and Advanced Engineering*, 2(7), 438–453.

Sahasrabudhe, S. S., and Nagarajaiah, S. (2005). “Semi-active control of sliding isolated bridges using MR dampers: an experimental and numerical study.” *Earthquake Engineering & Structural Dynamics*, 34(8), 965–983.

Skinner, R. ., Robinson, W. ., and McVerry, G. . (1993). *An introduction to seismic isolation*. *Wiley Publishers*.

Vasiliadis, L. K. (2016). “Seismic evaluation and retrofitting of reinforced concrete buildings with base isolation systems.” *Earthquakes and Structures*, Techno-Press, 10(2), 293–311.

Wang, Y.-P., Chung, L.-L., and Liao, W.-H. (1998). “Seismic Response Analysis Of Bridges Isolated With Friction Pendulum Bearings.” *Earthquake Engineering & Structural Dynamics*, 27(March), 1069–1093.

Wen, Y.-K. (1976). “Method for Random Vibration of Hysteretic Systems.” *Journal of the Engineering Mechanics Division*, ASCE, 102(2), 249–263.

Yang, J. N., Wu, J. C., Agrawal, A. K., and Li, Z. (1994). “Sliding Mode Control for Seismic-Excited Linear and Nonlinear Civil Engineering Structures.” *Technical Report NCEER-94-0017*, (june), National. Centre for Earthquake Engineering. Resea.

Yoshida, O., and Dyke, S. J. (2004). “Seismic Control of a Nonlinear Benchmark Building Using Smart Dampers.” *Journal of Engineering Mechanics*, 130(4), 386–392.

Yoshida, O., Dyke, S. J., Giacosa, L. M., and Truman, K. Z. (2003). “Experimental verification of torsional response control of asymmetric buildings using MR dampers.” *Earthquake Engineering & Structural Dynamics*, 32(June), 2085–2105.